Multi-scale analysis of the generated damage when machining pockets of 3D woven composite for repair applications using abrasive water jet process: Contamination analysis

Xavier Sourd, Redouane Zitoune, Akshay Hejjaji, Mehdi Salem, Laurent Crouzeix, D. Lamouche

Multi-scale analysis of the generated damage when machining pockets of 3D woven composite for repair applications using abrasive water jet process: Contamination analysis

X. Sourd [a,b,*], R. Zitoune [a,*], A. Hejjaji [a], M. Salem [c], L. Crouzeix [a], D. Lamouche [b]

[a] Institut Clément Ader, CNRS UMR 5312, 3 Rue Caroline Aigle, 31400 Toulouse, France
[b] Safran Aircraft Engines, Villaroche, Rond-point René Ravaud, 77550 Moissy-Cramayel, France
[c] Institut Clément Ader, CNRS UMR 5312, Campus Jarlard, 81013 Albi, France

Keywords:
A. Polymer-matrix composites (PMCs)
A. 3-Dimensional reinforcement
D. Surface analysis
E. Machining

A B S T R A C T

Repair of damaged aircraft structural parts is a regular maintenance activity carried out to preserve airworthiness while being economically viable. Conventional repair techniques used have negative impact on the repair quality and environment due to dust emission. For eliminating aforementioned problem, this study investigates controlled depth abrasive water jet (AWJ) milling for repair procedure of 3D woven CFRP composite structures used in the new aircraft engine developed by Safran Aircraft Engines. The aim is to identify and quantify the damage and surface contamination induced by AWJ milling. For this, the influence of milling parameters on the damage and surface contamination is investigated through full factorial experimental study. Several characterisation techniques like 3D optical profilometry, Scanning Electron Microscopy and X-ray tomography combined with image processing were used for a multi-scale analysis of the machined surface damage and contamination. In fact, the machining quality was quantified using an innovative criterion called "crater volume" (Cv). The obtained results have shown surface contamination by embedded abrasive particles and presence of bare and broken fibres, cracks, craters. The results show that the rate of contamination is influenced by the jet pressure and the scan step and the Cv is influenced by the jet exposure time.

1. Introduction

Due to the more and more stringent environmental rules provided by the aviation authorities, the aerospace industry has to drastically reduce the fuel consumption of the aircrafts. In order to achieve this goal, manufacturers decided to introduce advanced materials which have a high strength to weight ratio in the aircraft structure. To do so, they have developed cutting edge composite materials composed of polymer matrix and 3D woven fibres, used either for monolithic or multi-material structures. In service, these structures can be damaged, mainly by erosion or impact concerning outer parts, and are rather repaired than replaced during maintenance due to the high material and manufacturing prices. However, the repair procedure is subjected to strict guidelines provided by the maintenance and repair organizations (MRO), making it expensive for the aviation companies (aircraft grounding, highly skilled staff). In addition, as the composite repair are more and more performed by adhesive bonding, the quality of the machined surface is of primary concern to have a strong and enduring bonded repair. However, the quality of the machined surface is strongly influenced by the process of machining as well as the machining parameters [1–3]. In the industrial field, conventional machining is used for material removal to remove the damaged area. Nevertheless, Carbon Fibre Reinforced Plastics (FRPs) are difficult to machine properly because of their heterogeneous mechanical and thermal properties. In addition, due to the high abrasiveness of carbon fibres, important and premature tool wear is recorded during conventional machining of CFRPs, leading to high machining temperature and hence thermal degradation of the matrix, which has a low thermal conductivity compared to carbon fibres [4–6]. Another important drawback when machining CFRP by conventional means is the emission of harmful particles in the air, in form of carbon fibre dust, which is dangerous both for the environment and the operator's health [7,8]. Moreover, the main mechanical defects produced by conventional machining of CFRP are in form of delamination, broken fibres, fibre pull-outs and craters

* Corresponding authors.
E-mail addresses: xavier.sourd@iut-tlse3.fr (X. Sourd), redouane.zitoune@iut-tlse3.fr (R. Zitoune).

[4,5,9,10]. The location and expanse of all these defects mainly depend on the process parameters and the machining direction with respect to fibres orientation [11,12]. Both the thermal and mechanical defects can lead to a drop of the mechanical properties (endurance limit) of the structures in service [6,7,13].

Based on all these issues, the use of non-conventional machining processes has been considered for CFRPs, such as laser beam, electro-discharge or chemical machining. By removing the rigid tool in the process, cutting forces are considerably reduced, making the workpiece more easily positioned on the machining table. However, laser beam machining generates a high temperature, resulting in the presence of Heat Affected Zones (cracks, burns) and fumes which can be harmful for the operator if inhaled [14–16]. This process has also a low material removal rate compared to other techniques, increasing the machining time which is not suitable for economic reasons [17]. Electro-discharge machining produces also a high temperature, leading to large heat affected areas, and other defects as fibre swelling, delamination and recast material [18,19]. Moreover, this machining technique greatly depends on the material's conductivity, making more efficient for metallic materials applications. Chemical machining, currently employed for metal-composite structure machining applications, is a time consuming and dangerous process both for the operator's health and the environment because of the corrosive chemical products used. In order to avoid these issues, abrasive water jet (AWJ) machining has been suggested as a substitute non-conventional process. The water jet lowers the spread of carbon particles, by clearing out the chips and dust, and eradicates the heat affected zones [17,20]. Moreover, this machining process permits to remove a constant depth even on slightly curved parts [21,22], operation which can be complicated when machining is performed by conventional techniques. Numerous studies [17,22–25] have shown the versatility of AWJ which can machine a lot of different materials, such as titanium alloys and FRP laminates composites. To the authors knowledge, no study has been performed concerning AWJ machining on 3D woven composite, all the less the contamination phenomena of composites (unidirectional laminates, 2D and 3D woven fabrics) by abrasive grit. In addition, the mechanisms of material removal are independent on the fibres orientation because they are performed by micro-erosion consecutive to impact of the abrasive particles [26]. AWJ, by overcoming many drawbacks of conventional milling, seems then to be an interesting alternative process, especially in case of composite repair application in the aerospace field. However, as for all machining techniques, AWJ generates several kinds of defects. On one hand, it has been shown by Hejjaji et al. [22,25] that milling with this technique on CFRP laminates made of unidirectional plies induces defects and damage in form of broken fibres, fibre pull-out, fibre-matrix debonding, craters, abrasive embedment and grooves, which location and expanse depend on the choice of the machining parameters. All these defects are due to the material removal occurring mainly by micro-erosion of the matrix and brittle fracture of the fibres consecutive to solid impact of highly energetic abrasive particles [3,22,26–30]. On the other hand, the energy carried by water can favours delamination phenomenon by wedge effect if the parameters are not well chosen, which makes plain water jet machining unsuitable for composite milling. In case of AWJ, the abrasive flow rate must be carefully selected so the fraction of energy transferred from the water to the abrasive is important enough [21,24,31,32]. Besides, the high speed abrasive particles produce another kind of defect when impinging the machined surface. Once embedded in the target material, they introduce stress concentration zones which weaken the structure, by getting inside the cracks and avoiding them to close for example. As for the other types of defects, the degree grit embedment depends on the machining parameters – mainly on the energy transferred to the particles – and the milling path as well as the nature of the material [33,34]. Indeed, the machining strategy has to be properly designed in order to avoid sharp direction changes which can modify the erosion conditions and then worsen the surface quality. It is important to notice that the classical criteria used in industry to quantify the post-machining surface quality are the average surface roughness Ra and the surface waviness Wa. In case of AWJ milling of CFRP laminates, Hejjaji et al. [22,25] have shown that Ra depends on jet pressure and traverse speed in order of significance, with low influence of scan step. Likewise, the surface waviness of the milled specimens depends on scan step, jet pressure and traverse speed. However, surface roughness does not seem to be an efficient criterion to link surface quality and post-machining (conventional or non-conventional techniques) mechanical behaviour of CFRPs, both in static and fatigue, because of contradictory results [35–37]. In order to overcome this issue, another parameter has been considered, called "crater volume per unit area" (Cv). Contrarily to the classical parameter (Ra), Cv permits to take into account and quantify craters, the main defect encountered when machining composite with AWJ. Moreover, it has been proven than as the crater volume increases, the mechanical properties of the machined specimens are altered [22,35]. However, no work, to the authors' knowledge, has been performed concerning defects identification and quantification consecutive to AWJ milling on 3D woven composite specimens.

The goal of this work is then to identify and quantify the damage induced by abrasive water jet milling on 3D woven CFRP. The influence of the machining parameters of the process on the different nature and sizes of damage will be studied. To do so, specimens made of 3D woven CFRP have been milled following a full factorial experimental design of three machining parameters (viz. water jet pressure, traverse speed and scan step). After the milling phase and based on several characterisation techniques like 3D optical profilometry, Scanning Electron Microscopy (SEM) and X-ray tomography – a multi-scale analysis of the machine-induced damage with respect to the process parameters is discussed. A focus is made on grit embedment and the effect of the process parameters on the contaminated area. Finally, the "crater volume" parameter (Cv) expressed in terms of volume per unit area is used to quantify the machined surface defects.

2. Material and methods

2.1. Material

The tests of this study have been performed from a plate made of CFRP 3D woven composite. The epoxy resin and fibres constitutive of the material are respectively referenced as PR520 (Cytec Company) andIM7 (Hexcel Composites Company). The plate was manufactured by light Resin Transfer Molding process, having a thickness of 9.75 ± 0.04 mm and a nominal fibre volume fraction of approximately 54%. No further details (e.g. weaving architecture and mechanical behaviour) are presented due to the confidentiality of the material, which is the property of Safran Aircraft Engines. As seen from Fig. 1, the surface of the plate is rather flat (±30 μm from the 3D topography) with minor scratches due to handling and transportation. A full factorial design has been selected, with 36 specimens (140 mm × 20 mm), all originating from the same plate and obtained by abrasive water jet (AWJ) cutting. For each specimen, a given set of parameters (viz. pressure, traverse speed and scan step) was selected to mill by AWJ three identical pockets, of size 20 mm × 20 mm.

2.2. Abrasive water jet milling machine and parameters

All the machining operations (trimming and milling) were performed on an AWJ machine Mach 4c from *Flow* company. The different parameters (fixed and variable) selected for the tests are gathered in Table 1. Some parameters (such as the cutting head geometry) are fixed for economic reasons. The abrasive employed from the machining operations is a 120 mesh (around 125 μm in diameter) Arabian garnet produced by *Garnet Arabia Company Ltd* from Saudi Arabia. A single size of abrasive grit was kept for all the machining process due to limitation of the AWJ machine (only one abrasive feeding system available).

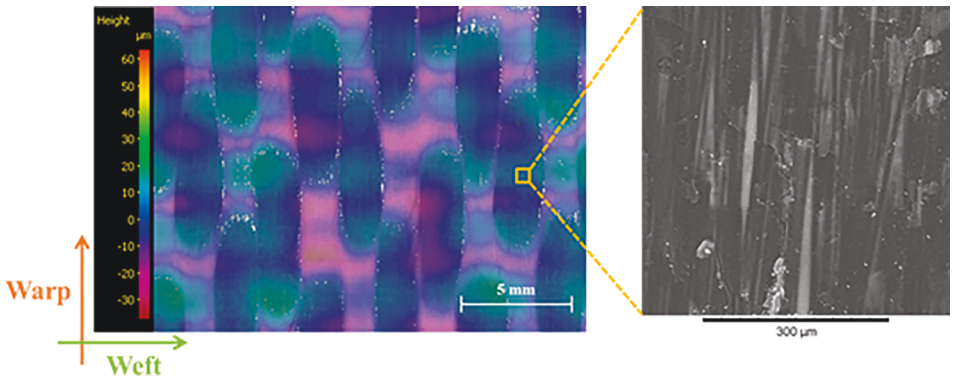

Fig. 1. Mixed view (optical and 3D topography) of the 3D woven CFRP composite plate. (For interpretation of the references to colour in this figure legend, the reader is referred to the web version of this article.)

Table 1
Fixed and variable parameters selected for the milling process.

Fixed parameters		Variable parameters	
Parameter	Value	Parameter	Levels
Focusing tube diameter	1.016 mm	Pressure P (MPa)	98/117/137/156
Focusing tube length	76 mm		
Nozzle diameter	0.3302 mm		
Type of abrasive	Garnet sand	Traverse speed V (m/min)	2/4/8
Abrasive size	#120		
Abrasive flow rate	0.18 kg/min	Scan step S (mm)	0.5/1.0/1.5
Standoff distance	100 mm		

According to Cénac et al. [38], there is an optimum value of the abrasive flow rate which, with a given geometry of the cutting head and especially the nozzle diameter, maximize the cutting depth. This optimization is of primary concern from the industrial point of view. Based on this paper and the nozzle used in the present study, the abrasive flow rate was fixed to 0.18 kg/min. Because the specimen's machining quality seems not to be significantly influenced by the standoff distance (SoD) [22,25], this parameter was set to 100 mm, value used by other authors [39,40] in case of milling with AWJ.

The variable parameters have been chosen thanks to the conclusion drawn from a review concerning milling with AWJ. Indeed, the water jet pressure, the cutting head's traverse speed and the scan step have been selected due to their greater influence on the pocket's geometry [22,26,41,42] compared to the other process parameters. Both traverse speed and scan step are studied through three different levels (cf. Table 1). The water jet pressure being considered as the most influential parameter on the surface quality of machining [22,25], four levels were taken (cf. Table 1). It has to be noted that a gap has been registered between the instruction sent to the machine and the effective pressure measured by the water jet machine's manometer during milling. This small variation in the pressure appears when the jet exits the nozzle and has been estimated around 17 MPa. In the results section, the effective value of the pressure is considered when mentioning "pressure". Of course, considering that the standoff distance is set to 100 mm, the jet is expected to expand significantly, at first sight making the use scan step values close to the nozzle diameter inconsistent to analyse the effect of this machining parameter on the contamination rate. However, the jet geometry has already been investigated in a previous study [43]. Indeed, the jet has been filmed with high speed camera which permitted to distinguish the two zones described previously. The primary jet, which carries the particles and then has the cutting role, has a diameter being estimated around 1.5 mm at 100 mm from the nozzle exit and for the jet pressures presented in this study. In addition, according to several works, [44,45], there is a Gaussian distribution of the grits within the jet. That is why the estimation of the "effective" jet diameter being close to the nozzle diameter, which is 1.016 mm, has been made, which justifies the chosen values of scan step chosen presented in Table 1. Following a full factorial design, 36 specimens, with three replicates, have been machined, hence 108 milled pockets.

Because of the lightness of the specimens, they needed to be clamped on the machining table so the water swirl did not make them move (cf. Fig. 2a). A raster scan pattern was considered as the pocket milling path with a machining direction parallel to the specimen's width. To avoid the disparity of erosion due to the speed variations, the changes of milling direction occurred outside the specimens (cf. Fig. 2b). With this safety distance of 60 mm, the traverse speed is stabilized throughout the milling process.

2.3. *Characterization methods*

2.3.1. *Topographies acquisition*

The topography of all the pockets were made thanks to optical profilometer Infinite Focus SL from *Alicona* (cf. Fig. 3) The measurements are performed with a technique called focus variation, acquiring the coordinates of each pixel centre of the scanned area by autofocus along the device's optical axis. Table 2 gathers the parameters used for the different measurements. The selected parameters allow a good compromise between acquisition precision (0.1 µm) and time (around 15 min for each scan).

2.3.2. *Surface quality and defects*

The machining quality was quantified thanks to the volume of craters produced during milling i.e. the volume between the mean least squares plane and the effective bottom surface. The mean plane used to calculate the crater volume is the same which has permitted to measure the mean depth of cut on a previous study [43]. Then, every void below this plane has been considered as over-erosion and qualified as "crater". No elimination of surface form has been performed before the calculation as the specimens are thick enough (9.75 mm) to avoid deformation consecutive to residual stress induced by machining. In addition, this mean plane is mathematically estimated by least squares method implemented in the post-processing software of Alicona profilometer. This technique was initially proposed by Hejjaji et al. when machining composite laminates made of unidirectional plies [22,25] and has proven to be a good estimator of the post-machining surface quality. The measurements have been performed thanks to the topology profiles from the profilometer. The scanned area is 14 mm × 14 mm on the pocket's bottom in order to avoid the edge effects consecutive to the jet entry and exit on the material. The volume of craters is then divided by the scanned surface in order to have a volume by unit area which is better for comparison between the specimens. The obtained results were

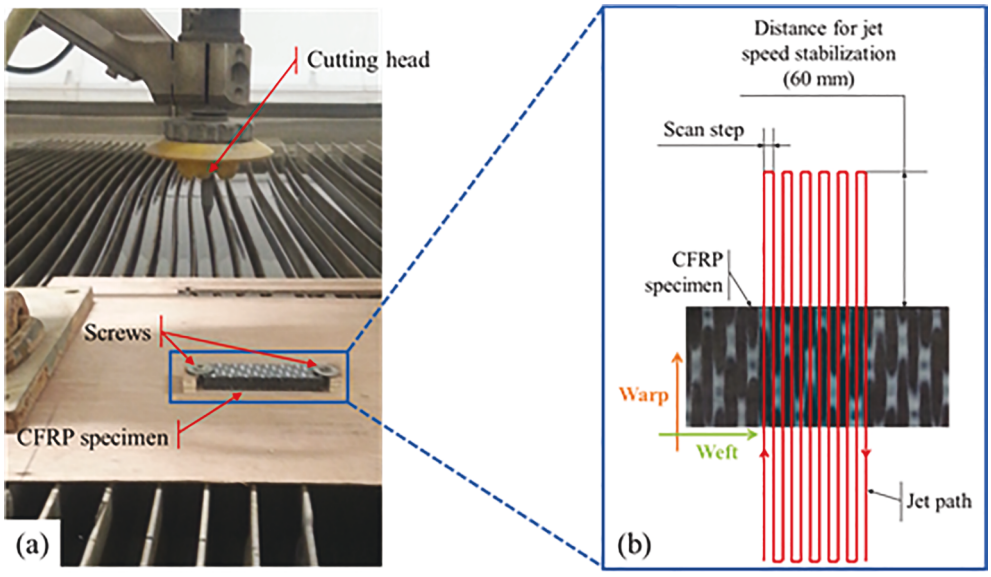

Fig. 2. (a) Set up of the machining operations and (b) Schematic top view of the milling path strategy. (For interpretation of the references to colour in this figure legend, the reader is referred to the web version of this article.)

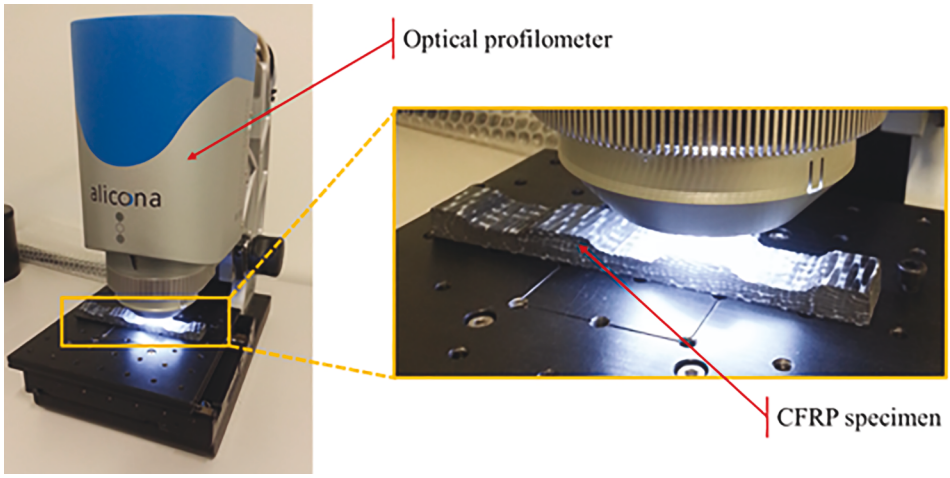

Fig. 3. Optical profilometer used for the topographies acquisition. (For interpretation of the references to colour in this figure legend, the reader is referred to the web version of this article.)

Table 2
Parameters used for the profiles and topographies acquisition.

Parameter	Value
Objective	10x
Vertical resolution (μm)	0.1
Lateral resolution (μm)	2.0
Scanned surface (mm^2)	16.8 × 16.8
Used surface (mm^2)	14.0 × 14.0

correlated with SEM images for identification and quantification of the surface damage. Moreover, some measurements with classical surface quality (surface roughness Ra and waviness Wa) have also been made from the topologies using the software provided by *Alicona*. Each line detailed on Fig. 4 corresponds to10 profiles separated by 4 μm. Two sets of three measurements have been performed, respectively in the warp direction along the jet path (L_1 to L_3) and in the weft direction perpendicularly to the jet path (T_1 to T_3). A Gaussian filter, with a cut-off length of 2.5 mm, has been used to separate the roughness from the waviness. The surface roughness and waviness in the warp (Ra_L and Wa_L) and weft ((Ra_T and Wa_T) directions of the reference surface (pre-water jet milled) are respectively $Ra_L = 1.77 \pm 0.27$ μm, $Wa_L = 3.79 \pm 0.37$ μm, $Ra_T = 1.45 \pm 0.17$ μm and $Wa_T = 3.65 \pm 0.69$ μm.

Scanning electron microscope (SEM) was used to find and identify various machining induced defects on the machined surface (cf. Fig. 5). SEM images obtained from secondary electron (SE) sensor at different magnification levels was used to identify the nature and form of various defects, in addition, back scattered electron (BSE) images were used to highlight the presence of abrasive particles stuck on the machined surface. Indeed, the BSE sensor differentiates various elements present on the studied surface based on their atomic number and hence produces a grey scale image of the surface where elements with lower atomic numbers are darker and vice versa. Based on the processing of these BSE images (ImageJ software), the contaminated area by the abrasive particles has been quantified which represents the ratio between the area taken up by the particles over the total area analysed by SEM viz. 5 mm × 5 mm which is considered as wide enough to capture the tow and resin rich regions.

X-ray tomography images have been performed with a Micro-Tomography Easy Tom 130 machine. A 360° exposure of the

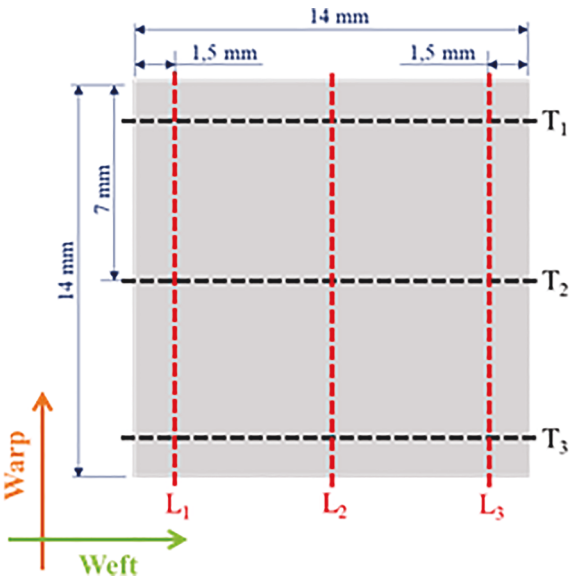

Fig. 4. Schematic view to illustrate the location of 2D profiles extraction for the Ra and Wa measurement from the topologies of machined surfaces (14 × 14 mm) for both directions "warp" (L_1 to L_3) and "weft" (T_1 to T_3). (For interpretation of the references to colour in this figure legend, the reader is referred to the web version of this article.)

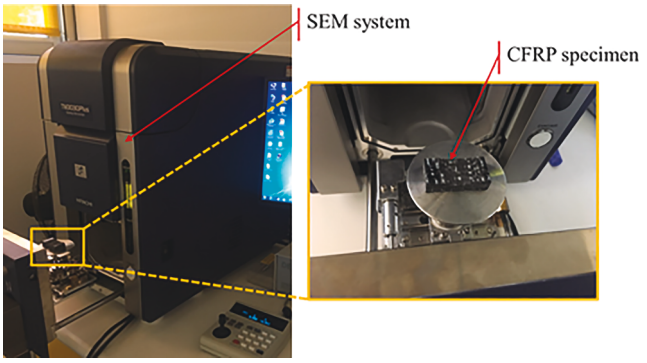

Fig. 5. Scanning Electron Microscope used for the observations of the milled surfaces. (For interpretation of the references to colour in this figure legend, the reader is referred to the web version of this article.)

specimens have permitted to obtain images from the three space plans. The distance between the specimen and the X-Ray source is around 3 cm. The X-ray current and voltage were respectively set to 100 mA and 80 kV. In addition, the source spot has a size of 3 mm. With these parameters, the maximum resolution of measurement was 25 μm.

3. Results and discussion

3.1. Types of defects

As mentioned in Section 2.3.2, the first thing to notice is that none of the specimens are distorted after pockets machining, contrarily to the results observed by Hejjaji et al. [22], after machining of CFRP specimens made of unidirectional plies. This difference can be explained by the fact that, on one side, the thickness of their specimens (around 2 mm) is way smaller than the one in the present study (around 9.75 mm), which implies a greater deformation of the specimens consecutive to residual stress induced by machining. On the other side, in the current study, pockets (20 mm × 20 mm) have been milled on specimens characterized by a dimension of 20 mm × 150 mm. However, in the work conducted by Hejjaji et al. [22], the milling zone concerns all the top surface of the specimens. In this case, the removal of some plies can modify the balance in the composite lay-up and then favour the distortion of the specimens. In addition, in the present study, the 3D weaving architecture leads to avoid this imbalance leading to flat surfaces. The material removal during AWJ milling is mainly by means of micro erosion caused by solid particle impact. This physical interaction between abrasive particles and the composite workpiece gives rise to a modified surface with several kinds of localised surface flaws. Therefore, Scanning Electron Microscope (SEM) was used to observe and identify various machining induced defects on the surface. However, the most prominent defect that was observed was large craters on the machined surface, which was visible to the naked eye and having an average diameter of 2 mm (cf. Fig. 6a). It is to be noted that these macro craters (red dotted circles in Fig. 6a) are created due to the fibre weaving architecture of the 3D composite. Contrarily to what is expected, the fibre tows (red dotted circles in Fig. 6b) on the 3D composite are more easily eroded by the AWJ than the white resin rich areas, hence giving rise to a crater of the similar size. This is due to the fact that the fibre tows are constitutive of discrete entities (fibres) which are easily broken by the abrasive particles. In this case, the material is removed by steps which depth is equal to the fibres diameter. On the opposite, the resin rich regions of the specimens (white zones in Fig. 6b) act like an homogeneous material which has to be eroded and/or cut.

Further, high magnification SEM analysis of the machined surface reveals several other micro size defects. The most prominent micro defect was bare and broken fibres. This defect was found across all specimens irrespective of the machining parameters. The bare fibres are the exposed fibre filaments due to removal of the matrix (cf. Fig. 7a). In addition, broken fibres were found all across the surface, especially near the walls of the macro craters (cf. Fig. 7b). Some fibres were broken due to longitudinal and transverse cracks (cf. Fig. 7c & d). By having a closer look on Fig. 7d, it can be noticed that some fibres are chipped, probably indicating the origin of particles impact. Cracks being located at the vicinity of these impact zones, it may be considered that they are the results of several smaller cracks, originating from these impact zones, which have merged. It has to be noted that Pahuja & Ramulu [46] also noticed exposed fibres as well fibre breaking in case of machining randomly chopped discontinuous fibre composites by abrasive water jet. This material is characterised, as it is the case in the present study, by resin rich regions.

Another major defect observed was microscopic craters, which can be termed as micro craters in order to differentiate from large craters (cf. Fig. 8). SEM analysis revealed that diameter of these microscopic craters ranged between of 80 μm and 200 μm and were randomly distributed across the machined surface irrespective of the machining parameters. They were also found on the bottom surface of the macro craters. These micro craters can form stress concentration zones and can be detrimental to the material integrity of the machined component.

Apart from these major defects matrix erosion and fibre matrix debonding was observed in some specimens (cf. Fig. 9). The occurrence of these defects was related to the jet traverse speed. As the jet traverse speed increased, the presence of debonding and matrix erosion was predominant. Similar results were reported by Hejjaji et al. [22] and it was attributed to the fact that the jet-workpiece interaction time is greatly reduced at higher traverse speeds. Hence the energy transfer time available to the abrasive particles is less, which means the jet stream is unable to remove the fibres effectively. However, the matrix being softer than the carbon fibres, comparatively lesser energy (only water) is enough to erode it. Therefore, at higher jet traverse speeds greater presence of debonding and matrix erosion is observed.

In addition, the X-ray tomography images have highlighted the presence of cracks up to 2 mm long which are perpendicular to the machined surface (cf. Fig. 10). It has to be noticed that these cracks are located close to the free edges of the specimens, were the jet enters the material. The analysis of the X-Ray images also reveals that the

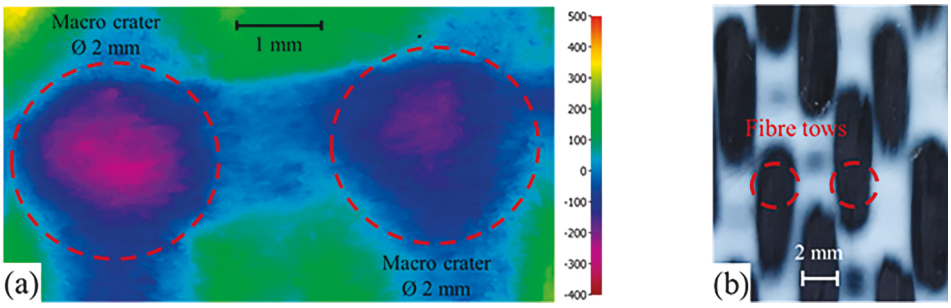

Fig. 6. (a) Topography image showing macro crater on the AWJ milled surface [P = 98 MPa/SS = 0.5 mm/V = 2 m/min] and (b) dimension of a single fibre tow in the 3D woven architecture. (For interpretation of the references to colour in this figure legend, the reader is referred to the web version of this article.)

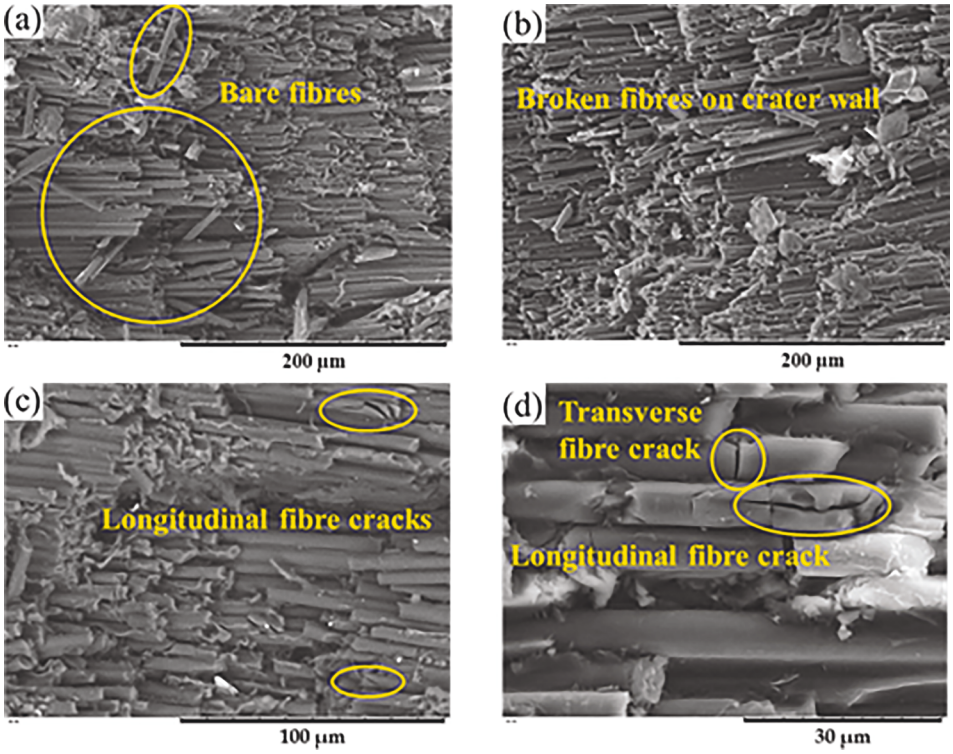

Fig. 7. Different kinds of microscopic defects on the AWJ milled surface, (a) Bare/exposed fibres, (b) broken fibres along the macro crater wall, (c) & (d) longitudinal and transverse fibre cracks. (For interpretation of the references to colour in this figure legend, the reader is referred to the web version of this article.)

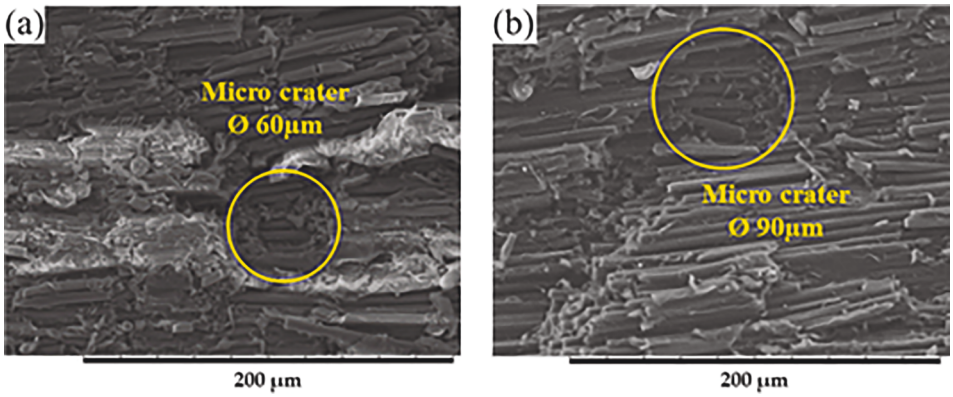

Fig. 8. SEM images showing craters of several sizes on the AWJ milled surface. (For interpretation of the references to colour in this figure legend, the reader is referred to the web version of this article.)

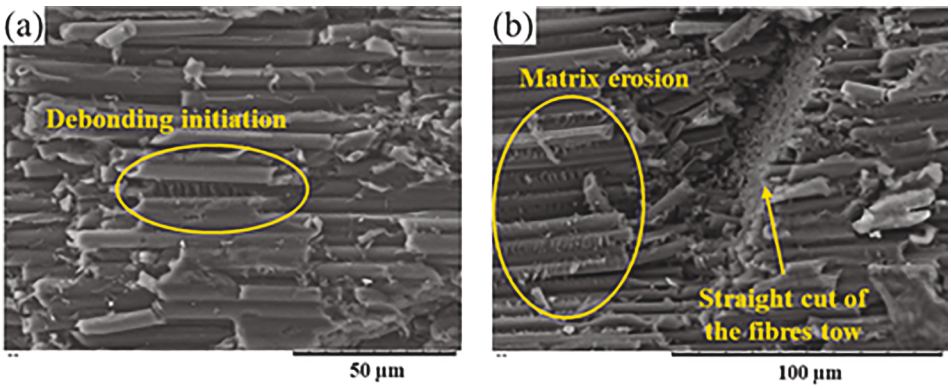

Fig. 9. SEM images showing (a) fibre-matrix debonding and (b) matrix erosion on the AWJ milled surface. (For interpretation of the references to colour in this figure legend, the reader is referred to the web version of this article.)

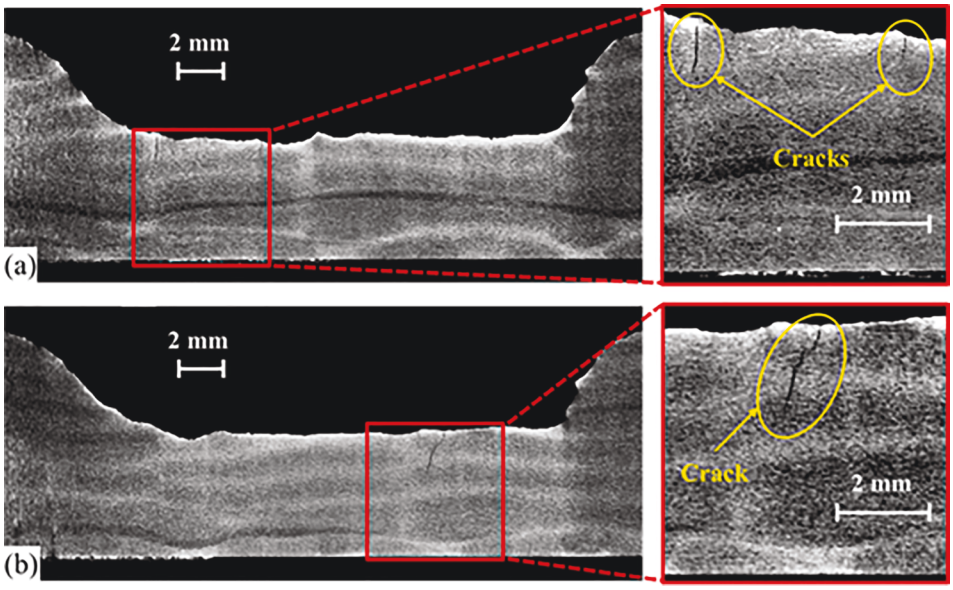

Fig. 10. X-ray tomography images showing cracks perpendicular to the surface throughout the milled zone close to both the free edges (a) and (b) of the specimens [P = 156 MPa/SS = 0.5 mm/V = 4 m/min]. (For interpretation of the references to colour in this figure legend, the reader is referred to the web version of this article.)

propagation depth of the cracks within the specimens is around 3 mm. As the cracks have been found along the pocket's free edge, it can be concluded that these defects originate from the entrance and exit of the water jet within the material during milling. No such defects have been found neither on the machined surface, nor along the free edges far from the pockets, which supports this conclusion.

Another major issue during AWJ milling was surface contamination due to embedment of abrasive particles in the machined surface. Abrasive particle embedment does not cause any physical material damage to the machined surface, hence this issue is dealt separately in the following section.

3.2. Quantification of the surface quality

3.2.1. Contamination

The abrasive particles (garnet sand) used for milling are harder than the matrix and the carbon fibres present in the composite workpiece. This can lead to surface contamination by embedment of the abrasive particles on the milled surface. Generally, loosely embedded particles are easily removed by the flushing action of the water jet (secondary jet), but some particles get fragmented after impacting the workpiece surface and these smaller fragments get deeply embedded in the matrix rich regions and the crevices formed between carbon fibres [46,47]. To investigate this phenomenon, scanning electron microscopy (SEM) was used in the back scattered electron (BSE) mode, where the obtained images show various levels of brightness depending on the atomic number of the element present. Hence, the heavier abrasive particles (containing Si and Al) appear lighter/brighter than the surrounding carbon fibres or matrix (cf. Fig. 11). Also, it can be noticed that the embedded abrasive particles (light areas in the Fig. 11) are smaller than the initial diameter of 125 µm (#120) and has sharp edges indicating that these are the fragments formed due to interactions inside the mixing chamber or after impacting the workpiece. Similar observations have been performed by Fowler et al. [33] in case of machining titanium alloy. The SEM-BSE images indicated that the smaller particles are embedded in between the fibres and cracks whereas larger ones are inside the micro craters. In the context of composite repair, the milled surface will be the parent surface on with the repair plies will be bonded using a suitable adhesive and when such contamination is present on the bonding surface it can lead to poor bonding and hence an inferior quality repair. Contrarily to metallic materials, a post-machining plain waterjet cleaning process cannot be performed on composite materials because of the great sensibility of the matrix to the water erosion [21,31] and only pressurized air can be used in order to remove the loose and lightly

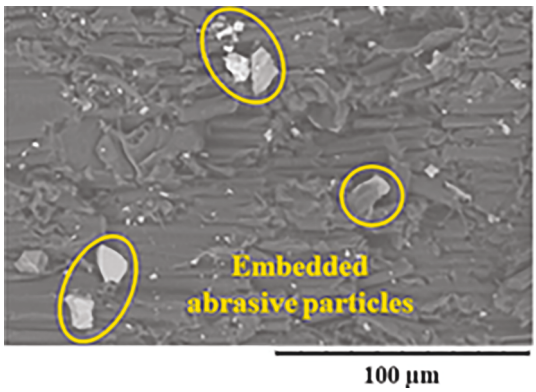

Fig. 11. Contamination of the milled surface by abrasive particles embedment [P = 98 MPa/SS = 1.5 mm/V = 4 m/min]. (For interpretation of the references to colour in this figure legend, the reader is referred to the web version of this article.)

embedded particles. Even with post machining air cleaning the abrasive particles are not removed in whole. Hence, the best way to reduce contamination is to use the machining parameters that leads to least contamination. In this context, the influence of machining parameters on the abrasive particle contamination is studied by analysing the SEM-BSE images (Greyscale Threshold tool in ImageJ) to obtain the contamination area in terms of percentage.

The effect of jet pressure and scan step on the abrasive particle contamination when machining at a traverse speed of 4 m/min is presented in the Fig. 12. It is clearly noticed that an increase in jet pressure induces lower levels of surface contamination. Indeed, at a scan step of 0.5 mm, the percentage of contaminated area drops from 0.8% to 0.2% for jet pressures of respectively 98 MPa and 137 MPa. From the flow mechanics studies, it is known that the abrasive water jet has two components: a primary jet which is the effective jet that carries abrasive particles and a secondary jet which is mostly water. This secondary jet does not contain abrasive particles and does not contribute to any cutting action. However, it aids in water erosion of the softer matrix material, meanwhile it also flushes the loose abrasive particles embedded in the matrix. Hence, with increasing pressure the flushing action of secondary jet increases too, reducing the contamination.

The Fig. 12 suggests that contamination increases with increasing scan step. However, a closer investigation by plotting the complete range of scan steps used for the studies reveals a different outcome. From the Fig. 13, it is clearly seen that the least contamination is obtained

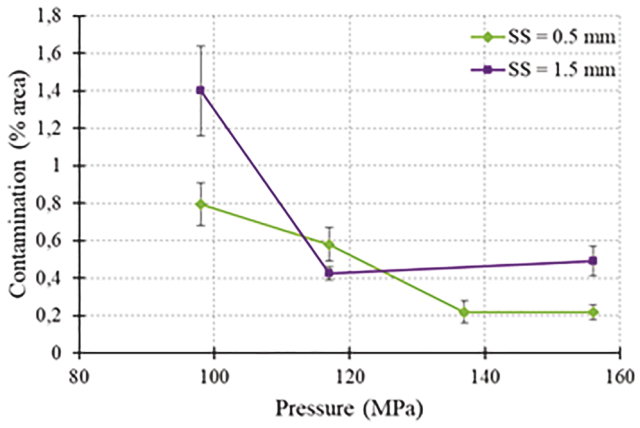

Fig. 12. Effect of the jet pressure and scan step on the percentage of contaminated area when machining is done with traverse speed of 4 m/min. (For interpretation of the references to colour in this figure legend, the reader is referred to the web version of this article.)

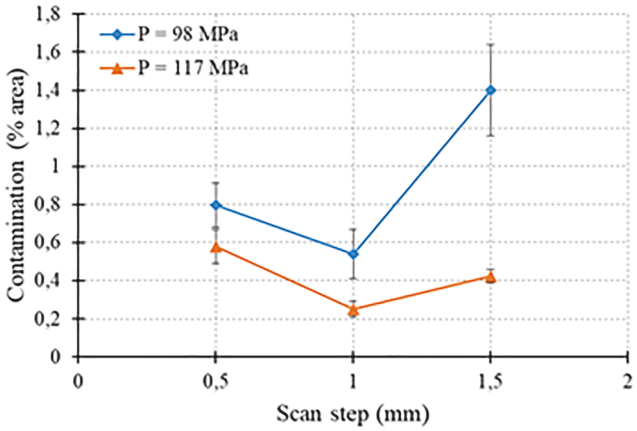

Fig. 13. Effect of the scan step on the percentage of contaminated area when machining is done with jet pressure of 98 MPa and 117 MPa and at traverse speed of 4 m/min. (For interpretation of the references to colour in this figure legend, the reader is referred to the web version of this article.)

when using a scan step of 1 mm irrespective of the pressure. As explained in Section 2.2, the effective jet diameter is considered to be close to the nozzle diameter used for the machining, which is 1.016 mm. Therefore, when the scan step is 1 mm, the adjacent jet traverse paths just brush each other and there is no overlapping or exclusion of the workpiece surface. Consequently, when the primary jet is removing material in its path, the secondary jet will be flushing out loosely embedded particles in the previous adjacent jet path leading to a lower contamination levels. However, when a scan step of 0.5 mm or 1.5 mm is considered, the adjacent jet paths overlap and isolate respectively. When the jet paths overlap (SS = 0.5 mm), milling occurs on already machined surface, leading to aggravate the formation of cracks and micro-craters where abrasive particle embedment occurs. Whereas, when the jet paths isolate each other (SS = 1.5 mm), the excluded region is mainly machined by the secondary jet which mostly erodes the matrix and creates crevices leading to abrasive particle embedment. In addition, due to the increased distance between adjacent traverse paths, the secondary jet would be weaker at that distance and the flushing action is ineffective. Hence, a higher jet pressure and scan step equal to the primary jet diameter is recommend for reducing abrasive particle contamination.

In addition, the influence of jet traverse speed on the contamination levels was not very clear. Though higher levels of contamination were found at low traverse speed (2 m/min) the contamination levels remained almost the same for the other speeds. Therefore, to get a clear affirmation, a wider range of speeds must be considered for the study. Finally, though all the machining parameters influence the degree of contamination, the values of contaminated areas are very low (around 1%), especially compared to metallic materials with similar sets of machining parameters (around 30% in case of machining of titanium alloy [34]).

3.2.2. *Surface damage and defects*

When dealing with surface quality, surface roughness (Ra) and waviness (Wa) are the most commonly used parameters. In the current study, this approach is not relevant as shown from Fig. 14. Each line detailed on the picture corresponds to10 profiles separated by 4 µm and the results are mean values obtained with a cutting length of 2.5 mm. A great disparity within the results, depending on the measured area and the direction of scanning, has been observed. Indeed, surface roughness and waviness of the machined surface vary respectively from 15.8 to 24.2 µm and 61.5 to 73.5 µm when measuring along the jet path (L_1 to L_3). Furthermore, in case of measuring perpendicularly to the jet path (T_1 to T_3), surface roughness and waviness vary respectively from 17.2 to 32.2 µm and from 35.0 to 62.0 µm. These scattered values can be mainly attributed to the weaving architecture of the specimen.

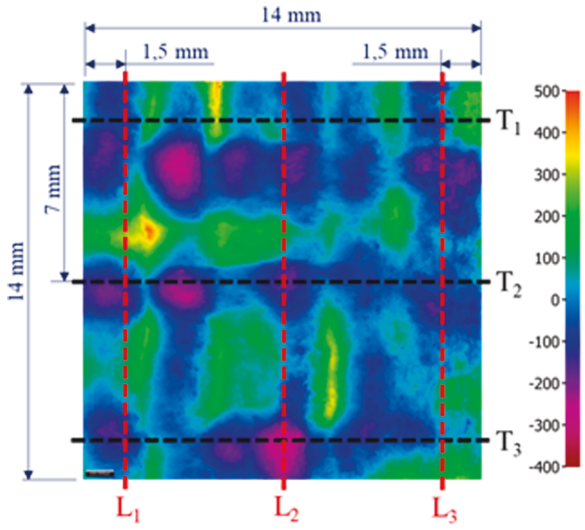

	Ra (µm)	Wa (µm)
L_1	17.8	73.5
L_2	24.2	67.7
L_3	15.8	61.5
T_1	32.2	49.1
T_2	17.2	35.0
T_3	20.2	62.0

Fig. 14. Topography and surface parameters (Ra, Wa) of a milled specimen [P = 98 MPa/SS = 0.5 mm/V = 2 m/min]. (For interpretation of the references to colour in this figure legend, the reader is referred to the web version of this article.)

Moreover, because of the local definition of both surface roughness and waviness, they do not take into account one of the most recorded type of defect on the specimens which is craters. In addition, several studies performed by Arola & Ramulu [48,49] have shown that the use of Ra to deduce the reduction in mechanical properties (both in static and fatigue) can be misleading when trimming Fibre Reinforced Plastics. Hence, it is necessary to find another criterion to quantify the surface quality.

As explained in Section 2.3.2, crater volume per unit area Cv is used in order to quantify the surface quality of the machined surface. Contrarily to other criteria, as surface roughness and waviness, Cv can take into account multi-scale defects such as craters. Moreover, this criterion permits to quantify the recessed volume consecutive to AWJ milling which can be an asset when considering post-machining operations such as bonding for example.

The mean effects of the milling parameters on the crater volume by unit area (Cv) are presented on Fig. 15. Each point of the graphs corresponds to a mean value of all specimens with similar set of parameters. For example, each point from Fig. 15a has the same set of pressure and traverse speed, with different scan steps. This parameter is then "hidden" and the focus is made on the combined influence of pressure and traverses speed.

It can be seen from Fig. 15a that the jet pressure greatly influences Cv in case of milling with low traverse speed (2 m/min). Indeed, when the pressure varies from 98 MPa to 156 MPa, the crater volume per unit area increases from 4.46 mm^3/cm^2 to 6.13 mm^3/cm^2. Milling with a low traverse speed leads to a long jet exposure time on the specimen. Because of the material's inhomogeneity, the matrix being more easily removed by the abrasive waterjet than the fibres, the disparity of removal is increased. The higher the jet energy (e.g. the higher the pressure), the greater this difference. By increasing the traverse speed, the effect of pressure on Cv is significantly reduced. This seems to prove that the jet exposure time is of crucial importance when considering the surface quality. Moreover, as the traverse speed increases, the crater volume slightly decreases, from around 4.7 mm^3/cm^2 to 4.0 mm^3/cm^2 for traverse speeds of respectively 4 m/min and 8 m/min.

The results from Fig. 15b emphasize the effect of scan step on the surface quality. Indeed, milling with a scan step smaller than the jet diameter (e.g. 0.5 mm) leads to an increase of craters as the pressure increases. Indeed, when the pressure increases from 98 MPa to 156 MPa, Cv rises from 4.43 mm^3/cm^2 to 5.92 mm^3/cm^2. This trend can be explained by the important degree of overlapping of two consecutive trenches when milling with a scan step of 0.5 mm. The defects created by a jet pass are worsen by the next one, reducing the surface quality. On the contrary, milling with a scan step around the nozzle diameter (1 mm) leads to an almost constant surface quality, which can be attributed

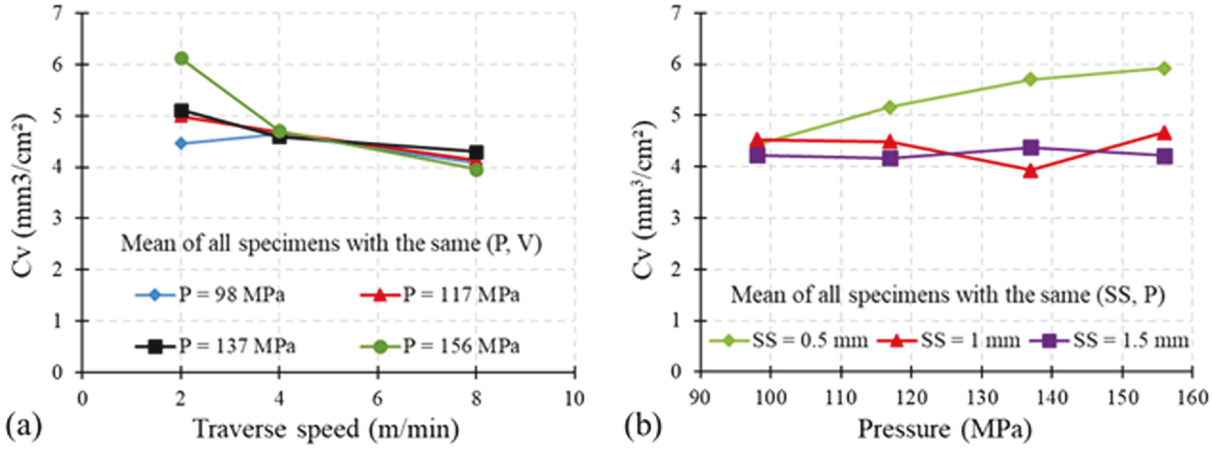

Fig. 15. Mean combined effect of (a) pressure and traverse speed and (b) pressure and scan step on the crater volume by unit area Cv. (For interpretation of the references to colour in this figure legend, the reader is referred to the web version of this article.)

to the bare and broken fibres as well as the macro craters originating from the weaving architecture observed on every milled specimen, whatever the pressure is. In this case, the already milled material is not furtherly removed as only the secondary jet, which has no cutting action, overlaps the previously machined material. The same trend observed with a scan step of 1.5 mm tends to show that the effective nozzle diameter is a bit greater than expected. Indeed, after measurement, it was found that the diameter is around 1.2 mm, due to erosion wear. This consolidates the above explanations.

4. Conclusion

The experimental study of AWJ milling of 3D woven CFRP was presented in this paper. The defects and damage consecutive to machining have been quantified thanks to the crater volume which has proven to be an effective method. Based on the obtained results, the following conclusions can be drawn:

- At macro level and for any machining conditions, large craters with a diameter around 2 mm, are observed. The dimensions of these craters can be related to the mesh of the weaving architecture of the composite specimens. However, at micro level, several types of damage have been highlighted. Indeed, the major defect, present on all the specimens scanned with the SEM, is in form of bare and broken fibres. When milling with high speed, due the limited exposure time, only the matrix is eroded which initiates fibre-matrix debonding. In addition, smaller craters have been noticed within the macro craters walls.
- Grit embedment has also been observed for all the milled specimens, whose rate depends on the machining parameters. Indeed, the increase of the jet pressure leads to a decrease of the contamination rate, due to the higher influence of erosion by water, which jets out the embedded particles and cleans the surface. Similarly, as the traverse speed increases, the jet exposure time on the workpiece decreases, hence also the contaminated area. Based on the SEM images, embedded grits within the composite material are located between fibres or inside cracks. However, though all the machining parameters influence the rate of contamination, the recorded values are way inferior to the ones estimated on metallic materials. This might mean that no heavy additional cleaning process is needed in order to have a surface suitable secondary purposes like bonding applications.
- Based on the topographies of the machined surfaces of the 3D composite material, it was clearly observed that the jet pressure combined with the jet exposure time, through the traverse speed and scan step, are greatly influencing the crater volume (Cv). This parameter (Cv) has then proven to be an efficient indicator to quantify the surface defects and damage consecutive to the AWJ milling process. Indeed, multi-scale analysis performed by SEM image processing on specimens with different process parameters consolidate the Cv measurements. However, it can be noticed that Cv does not take into account the problem of abrasive particle embedment, which can fill in the carters generated by the AWJ milling process, hence reducing the value of Cv.

CRediT authorship contribution statement

X. Sourd: Methodology, Software, Validation, Formal analysis, Investigation, Writing - original draft, Visualization. **R. Zitoune:** Conceptualization, Resources, Data curation, Writing - review & editing, Supervision. **A. Hejjaji:** Formal analysis, Investigation, Data curation, Writing - review & editing. **M. Salem:** Formal analysis, Investigation, Resources. **L. Crouzeix:** Resources, Writing - review & editing, Supervision. **D. Lamouche:** Conceptualization, Resources, Writing - review & editing, Supervision.

Declaration of Competing Interest

The authors declare that they have no known competing financial interests or personal relationships that could have appeared to influence the work reported in this paper.

Acknowledgments

The collaboration with Safran Aircraft Engines is gratefully acknowledged.

References

[1] Wang DH, Ramulu M, Arola D. Orthogonal cutting mechanisms of graphite/epoxy composite. Part I: unidirectional laminate. Int J Mach Tools Manuf 1995;35(12):1623–38.
[2] Wang DH, Ramulu M, Arola D. Orthogonal cutting mechanisms of graphite/epoxy composite. Part II: multi-directional laminate. Int J Mach Tools Manuf 1995;35(12):1639–48.
[3] Arola D, Wang DH, Ramulu M. Chip formation graphite/epoxy in orthogonal trimming of composite. Composites 1996;27:121–33.
[4] König W, Wulf Ch, Graß P, Willerscheid H. Machining of Fibre Reinforced Plastics. CIRP Ann 1985;34(2):537–48.
[5] Nguyen-Dinh N, Hejjaji A, Zitoune R, Bouvet C, Crouzeix L. Machining of FRP composites: surface quality, damage, and material integrity: critical review and analysis. Futur. Compos. 2018.
[6] Nguyen-Dinh N, Zitoune R, Bouvet C, Leroux S. Surface integrity while trimming of composite structures: X-ray tomography analysis. Compos Struct 2019;210:735–46.
[7] Haddad M, Zitoune R, Eyma F, Castanie B. Study of the surface defects and dust generated during trimming of CFRP: Influence of tool geometry, machining parameters and cutting speed range. Compos A Appl Sci Manuf 2014;66:142–54.
[8] Ramulu M, Kramlich J. Machining of fiber reinforced composites: Review of environmental and health effects. Int J Environ Conscious Des Manuf 2004;11:1–19.
[9] Koplev A, Lystrup Aa, Vorm T. The cutting process, chips, and cutting forces in machining CFRP. Composites 1983;14(4):371–6.
[10] Voss R, Seeholzer L, Kuster F, Wegener K. Influence of fibre orientation, tool geometry and process parameters on surface quality in milling of CFRP. CIRP J Manuf Sci Technol 2017;18:75–91.
[11] Janardhan P, Sheikh-Ahmad J, Cheraghi H. Edge Trimming of CFRP with Diamond Interlocking Tools. SAE Tech Pap Ser 2006.
[12] Sheikh-Ahmad J, Urban N, Cheraghi H. Machining damage in edge trimming of CFRP. Mater Manuf Processes 2012;27(7):802–8.
[13] Haddad M, Zitoune R, Eyma F, Castanié B. Influence of machining process and machining induced surface roughness on mechanical properties of continuous fiber composites. Exp Mech 2015;55(3):519–28.
[14] Leone C, Papa I, Tagliaferri F, Lopresto V. Investigation of CFRP laser milling using a 30W Q-switched Yb:YAG fiber laser: effect of process parameters on removal mechanisms and HAZ formation. Compos A Appl Sci Manuf 2013;55:129–42.
[15] Hejjaji A, Singh D, Kubher S, Kalyanasundaram D, Gururaja S. Machining damage in FRPs: laser versus conventional drilling. Compos A Appl Sci Manuf 2016;82:42–52.
[16] Herzog D, Jaeschke P, Meier O, Haferkamp H. Investigations on the thermal effect caused by laser cutting with respect to static strength of CFRP. Int J Mach Tools Manuf 2008;48(12-13):1464–73.
[17] Hashish M. An investigation of milling with Abrasive-Waterjets. J Eng Ind 1989;111:158.
[18] Sheikh-Ahmad JY. Hole quality and damage in drilling carbon/epoxy composites by electrical discharge machining. Mater Manuf Processes 2016;31(7):941–50.
[19] Holmberg J, Berglund J, Wretland A, Beno T. Evaluation of surface integrity after high energy machining with EDM, laser beam machining and abrasive water jet machining of alloy 718. Int J Adv Manuf Technol 2019;100(5-8):1575–91.
[20] Ramulu M, Kunaporn S, Arola D, Hashish M, Hopkins J. Waterjet machining and peening of metals. Analyzer 2000;122:90–5.
[21] Cénac F, Collombet F, Zitoune R, Déléris M. Abrasive-water-jet blind-machining of polymer matrix composite materials. ECCM 2008.
[22] Hejjaji A, Zitoune R, Crouzeix L, Roux SL, Collombet F. Surface and machining induced damage characterization of abrasive water jet milled carbon/epoxy composite specimens and their impact on tensile behavior. Wear 2017;376-377:1356–64.
[23] Arola D, Ramulu M. Material removal in abrasive waterjet machining of metals Surface integrity and texture. Wear 1997;210(1-2):50–8.
[24] Hashish M. Waterjet machining of advanced composites. Mater Manuf Processes 1995;10(6):1129–52.
[25] Hejjaji A, Zitoune R, Crouzeix L, Collombet F, Le Roux S. Impact of the abrasive water jet milling process on the damage and surface characteristics of CFRP composite. In: ECCM 2016 – Proceeding 17th Eur Conf Compos Mater; 2016.
[26] Hocheng H, Tsai HY, Shiue JJ, Wang B. Feasibility study of abrasive-waterjet milling of fiber-reinforced plastics. J Manuf Sci Eng 1997;119:133–42.

[27] Ramulu M, Arola D. The influence of abrasive waterjet cutting conditions on the surface quality of graphite/epoxy laminates. Int J Mach Tools Manuf 1994;34(3):295–313.
[28] Momber AW, Kovacevic R. Geometry, Topography and Integrity of Abrasive Water-Jet Machined Parts. In: Springer, editor. Princ abras water jet mach; 1998. p. 230–83.
[29] Sheldon GL, Finnie I. The mechanism of material removal in the erosive cutting of brittle materials. J Eng Ind 1966:393–9.
[30] Ramulu M, Arola D. Water jet and abrasive water jet cutting of unidirectional graphite/epoxy composite. Composites 1993;24(4):299–308.
[31] Cénac F, Collombet F, Zitoune R, Déléris M. Respect de l'intégrité dans l'usinage non-débouchant par jet d'eau abrasif de matériaux composites = Material integrity maintain while milling composite using abrasive water jet. JNC16, Toulouse, France; 2009.
[32] Shanmugam DK, Nguyen T, Wang J. A study of delamination on graphite/epoxy composites in abrasive waterjet machining. Compos A Appl Sci Manuf 2008;39(6):923–9.
[33] Fowler G, Shipway PH, Pashby IR. A technical note on grit embedment following abrasive water-jet milling of a titanium alloy. J Mater Process Technol 2005;159(3):356–68.
[34] Huang L, Kinnell P, Shipway PH. Parametric effects on grit embedment and surface morphology in an innovative hybrid waterjet cleaning process for alpha case removal from titanium alloys. Procedia CIRP 2013;6:594–9.
[35] Hejjaji A, Zitoune R, Toubal L, Crouzeix L, Collombet F. Influence of controlled depth abrasive water jet milling on the fatigue behavior of carbon/epoxy composites. Compos A Appl Sci Manuf 2019;121:397–410.
[36] Ghidossi P, El Mansori M, Pierron F. Edge machining effects on the failure of polymer matrix composite coupons. Compos A Appl Sci Manuf 2004;35(7-8):989–99.
[37] Squires CA, Netting KH, Chambers AR. Understanding the factors affecting the compressive testing of unidirectional carbon fibre composites. Compos B Eng 2007;38(4):481–7.
[38] Cenac F, Zitoune R, Collombet F, Deleris M. Abrasive water-jet milling of aeronautic aluminum 2024-T3. Proc IMechE 2015;229(1):29–37.
[39] Cénac F, Collombet F, Zitoune R, Déléris M. Usinage des Composites par Jet d'eau Abrasif. JNC17 2011.
[40] Zitoune R, Collombet F, Cénac F. Méthodologie spécifique à l'usinage des composites par jet d'eau abrasif. Tech l'ingénieur 2013.
[41] Kanthababu M, Ram M R, Emannuel Peter N, Gokul R, Rammohan R. Experimental investigations on pocket milling of titanium alloy using abrasive water jet machining. FME Trans 2016;44(2):133–8.
[42] Billingham J, Miron CB, Axinte DA, Kong MC. Mathematical modelling of abrasive waterjet footprints for arbitrarily moving jets: Part II—Overlapped single and multiple straight paths. Int J Mach Tools Manuf 2013;68:30–9.
[43] Sourd X, Zitoune R, Crouzeix L, Salem M, Charlas M. New model for the prediction of the machining depth during milling of 3D woven composite using abrasive waterjet process. Compos Struct 2020;234:111760. https://doi.org/10.1016/j.compstruct.2019.111760.
[44] Balz R, Heiniger KC. Determination of spatial velocity distributions of abrasive particles in abrasive water jets using laser-induced fluorescence under real conditions. WJTA-IMCA Conf Expo 2011.
[45] Lozano Torrubia P, Axinte DA, Billingham J. Stochastic modelling of abrasive waterjet footprints using finite element analysis. Int J Mach Tools Manuf 2015;95:39–51.
[46] Pahuja R, Ramulu M. Machinability of randomly chopped discontinuous fiber composites: a comparative assessment of conventional and abrasive waterjet. 23rd Int Conf Water Jet 2016;2016:127–48.
[47] Momber AW, Kovacevic R. Material-removal mechanisms in abrasive water-jet machining. Princ Abras Water Jet Mach 1998:89–162.
[48] Arola D, Ramulu M. Net shape manufacturing and the performance of polymer composites under dynamic loads. Exp Mech 1997;37(4):379–85.
[49] Arola D, Ramulu M. An examination of the effects from surface texture on the strength of fiber reinforced plastics. J Compos Mater 1999;33(2):102–23.